Chapter 6: Energy Storage Sizing for Plug-in Electric Vehicle Charging Stations

I Safak Bayram*, Ryan Sims**, Edward Corr**, Stuart Galloway*, and Graeme Burt*
*Department of Electronic and Electrical Engineering, Faculty of Engineering, University of Strathclyde, Glasgow, United Kingdom
**Power Networks Demonstration Centre, University of Strathclyde, Glasgow, United Kingdom

Chapter Abstract

To support, plug-in electric vehicle (PEV) growth, there is a need to design and operate charging stations without increasing peak system demand. In this chapter, first, an overview of on-going demonstration and testing studies are presented to show the complexity of the actual charging infrastructures and uncertainties related to customer demand. Then, an analytical model for a large-scale charging station with an on-site energy storage unit is introduced. The charging system is modelled by a Markov-modulated Poisson Processes with a two-dimensional Markov chain. A Matrix geometric based algorithm is used to solve steady state probability distribution to compute optimal energy storage size. Case studies are presented to show (i) the relationships between energy storage size, grid power and PEV demand and (ii) how on-site storage can reduce peak electricity consumption and the station's monthly electricity bill.

Keywords- Plug-in Electric Vehicle Charging Station, Energy Storage Systems, Demand Charge Management, Stochastic Modelling, Markov Processes

6.1. Introduction

The future of electric power grids is currently shaped by two major advancements, namely higher use of renewables on the supply side and increasing adoption of PEVs on the demand-side. These advancements aim to decarbonize electricity and transportation networks since

more than half of the global energy-related carbon emissions are attributed to these two sectors. The push towards PEVs is supported by legislations and regulations to encourage PEV uptake. For instance, a number of countries including the United Kingdom, France, and Norway plan to phase out fossil fuel cars by introducing a ban on the sale of such vehicles and increase the coverage of charging network within the next two decades (Tajer, 2017). On the other hand, reaching net zero goals would require an exponential adoption of PEVs; for instance, in the UK there are currently two hundred thousand PEVs on the road and this number needs to be around four million by 2030 to meet government policies (Haslett, 2019). Similarly, the State of California has a mandate to acquire one and half million PEVs by 2025 and generate half of its electricity with renewables by 2030. Net zero policy impacts are visible in France as there is a spring-back effect on the year-on-year (January 2019-2020) PEV market share jump from 2.7% to 11%. To that end, after being considered as a fringe technology, PEV market is getting closed to a tipping point (Sperling, 2018). This can be viewed in PEV sales and forecasts as shown in Figure 6.1

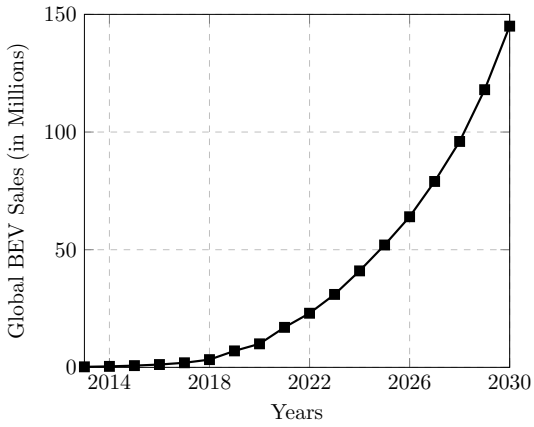

Figure 6.1 Battery electric vehicle (BEV) sales and forecasts (International Energy Agency) (https://www.iea.org/reports/global-ev-outlook-2019, 2019)

To support electrification of transportation, there is a need to deploy charging nodes to meet various customer needs shaped by time, location, and duration of service. In this chapter, we

present a large-scale PEV charging lot architecture equipped with an on-site storage unit. The primary goal is to develop a probabilistic method to optimally size storage unit and show how on-site storage can be effective in reducing peak demand and operational costs. Furthermore, we present an overview demonstration studies conducted at Power Networks Demonstration Centre[1] on PEV charging infrastructures.

At the moment, there are three typical charging options for PEVs (Falvo, 2014). First option is level 1 charging which takes place in customer's premises. Level 1 charging uses existing, typically single phase, electrical circuit at residential units (2-3 kW) and fills the PEV battery during the night. Second charging option uses AC level 2 chargers which are typically located at public parking lots (e.g., workplaces, shopping malls, etc.). This type of chargers typically supplies 6 to 7 kW power to stationary vehicle. Third option is called fast or ultra-fast charging which can transfer DC power at a rate of 50 kW – 350 kW (Srdic, 2019). Note that a typical fast model (50 kW) can deliver enough charge for a 100-mile trip with 30 minutes of charging, while ultrafast models are more preferred by high-end PEVs with large batteries. In this chapter, the proposed model employs level 2 chargers to serve cars parked at a large-scale lot. The related literature can be classified as three groups. First group of studies relate to smart charging (see Section 6.2.1) which is aimed at mitigating disruptive impacts of PEV demand on the power grid by exploiting the demand flexibility of PEVs. Second group of studies relate to design of charging stations and are categorized according to technology and economic operation domains (see Section 6.2.2). Third group is related probabilistic modeling of charging stations (see Section 6.2.3).

6.2. Literature Review

6.2.1. Literature on Smart Charging and Impacts of PEV Charging

Smart charging of PEVs is critical in transition towards electric transportation. Existing electric power grids are not designed to serve large PEV loads and concurrent charging of PEVs will lead to major technical challenges on the distribution, transmission, and generation components. At the distribution level, clusters of PEV load during peak hours can lead to premature aging of transformers, increase distribution system losses, and deteriorate power quality (J. García-Villalobos, 2014). Increased stress and voltage fluctuations will further risk the consistency and safety of the network. According to a field study conducted in the UK (Cross, 2016), one third of the low voltage feeders will require intervention when 40-70% of residents have PEVs. At the transmission level, PEV load increases transmission congestion level which is a major challenge as the investments towards new transmission lines have been declining. To support increasing electrification demand, there is an urgent need to expand transmission network capabilities (Jurgen Weiss, 2019). Finally, at the generation level, uncontrolled PEV load could lead to an increase in peak system load which requires system additional deployment of new system upgrades (Tehrani, 2015). To overcome aforementioned disruptive impacts, design and operation of charging facilities play a key role in transition to electric transportation.

PEVs are considered as new kind of electric loads that have both temporal and charging power flexibility. When a PEV is connected to a charger, charging session starts at a constant power. In the case of multiple PEVs connected simultaneously, they collectively increase peak loading and potentially trigger aforementioned disruptions. Smart charging is the optimization of charging power by exploiting PEV flexibility to maximize one or more benefits such as reducing peak load, increasing renewable energy utilization, lowering the cost of PEV charging, or deferring infrastructural upgrades (J. García-Villalobos, 2014). Smart charging can be implemented through standards such as IEC 61851 and ISO 15110 that enable control

and communication between charger and the vehicle. In addition, a group of PEV owners, coordinated by an aggregator, can participate in ancillary energy markets to stabilize electricity grids and, in return, receive payments for services rendered (Han, 2010). Vehicle-to-grid (V2G) applications are particularly important to smoothen what is known as solar "Duck Curves" which is used to define net electricity generation curve when there is significant solar generation. In this case, PEVs' charging rate are adjusted in a way to minimize the ramping up requirements of traditional power generators and lower financial losses (Lee, 2019).

6.2.2. Literature on Charging Station Design

The approach described in this chapter focuses on economic operation of charging stations and energy storage sizing (S. Negarestani, 2016) (M. R. Sarker, 2018). In this type of works, a critical component is local storage unit which is typically employed to shave peak load, reduce demand charges, and provide additional income via energy market participation. In (S. Negarestani, 2016), an optimal sizing approach is proposed for energy storage systems (ESSs) in fast charging stations. In this work, PEV demand is calculated based on driving patterns and optimal storage size is determined based on cost minimisation. In (M. R. Sarker, 2018), an optimisation framework is presented for an optimal bidding strategy in day-ahead electricity markets for a PEV charging station with an on-site storage. In the current charging station applications, the one of the main issues is related to expensive demand charges that constitute a sizable portion of monthly electricity bills and reduces station profits (The 50 states of electric vehicles, 2018). Demand charges are pricing tools to limit peak consumption of large customers by inducing a fee commensurate to the peak consumption during any fifteen minutes during each month. In June 2016 a charging facility with two fast-chargers, the following bill was issued (Ismail, 2019). The energy charge was 284 USD and demand charges for the peak power was more than 2900 USD, representing 91% of the total operational cost. High demand

charges both compromise business models and negatively impact PEV sales if prices are reflected to customers.

6.2.3. Literature on Probabilistic Modelling of PEV Charging Infrastructures

Since the experimentation of capital-intensive PEV charging stations is not possible, analytical modeling of PEV charging demand and infrastructure are used to provide insights to system planners in how different system components interact with each other. In line with the previous discussion, economic operation of charging infrastructures has been the topic of several mathematical modeling and optimization research works. Stochastic modeling and queuing systems have been widely used as such methods capture the probabilistic nature of problem related to different battery packs, technologies, weather parameters, and customer arrival and departure processes (Hu, 2016). Moreover, station may have uncertainties related to renewable energy output and storage unit can be modelled as a linear for simplification or non-linear "buffer" if battery's chemical dynamics are taken into account. Some of the related studies can be enumerated as follows. In (Aveklouris, 2017), fluid approximation of queueing models is adopted to calculate charging station overloading probabilities. In (E. Ucer, 2019), a queueing model is employed to calculate waiting times and service quality for a number of charging stations located in Ohio by using actual traffic traces. In (P. Fan, Operation analysis of fast charging stations with energy demand control of electric vehicles, , 2015), a charging station is modeled using a queuing model and captured the effect of constant current constant voltage charging on customer waiting times in the station. Customer arrival and charging demand statistics are important system parameters in charging stations. In (Fotouhi, 2019), using actual PEV charging data (level 2 chargers)

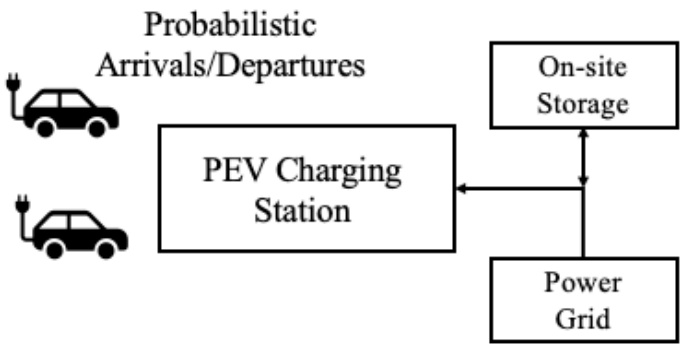

Figure 6.2 System overview

from a major North American University Campus between 2010-2015, a Markovian model for representing the charging behavior of PEV owners is presented. The results show that PEV owners not necessarily fully charge their batteries, hence, service duration is shorter than expected. In (Bayram, 2014), shared-based ESS located at residential units is modeled using fluid dynamic approach and storage sizing problem is solved by computing outage probability that of the system that is defined as the event when the load is higher than the supply.

6.2.4. Contributions

The contributions of this chapter can be enumerated as below:

- First, an actual demonstration and testing platform of a PEV charging infrastructure is introduced to show a detailed overview of a PEV charging infrastructure and sample measurement results.
- Second, a probabilistic system model for large scale PEV charging station equipped with an on-site energy storage is presented (shown in Figure 6.2). By considering the probabilistic nature of the customer demand, the proposed architecture is modelled by a Markov-modulated Poisson Process.

- Third, a matrix-geometric based algorithm is presented in detail and used to solve the associated capacity planning problem to find optimal energy storage size and station capacity respect to customer demand statistics.
- Fourth, practical case studies are developed to show that (i) by accounting for the statistical variations in customer demand, the power required for the station is significantly less than the sum of chargers' rated power and (ii) on-site storage units can help station operators to significantly reduce their electricity bills.

6.3. Demonstration and Testing Platform of a PEV Charging Infrastructure

Before presenting an analytical model for a large-scale charging station, an overview of an actual small-scale PEV charging station with associated hardware and software components are presented to provide a better understanding of actual system components. The Power Networks Demonstration Centre (PNDC) has completed several research projects relating to the electrification of transport and charging infrastructure. This includes electrical impact assessments of wireless inductive charging, on-street pop-up charger performance testing, and active power quality compensation of single-phase harmonic and load imbalance impacts of EV charge points. The PNDC was founded with the goal of accelerating the penetration of disruptive technologies from early stage research into business as usual adoption by the electricity industry. The facility comprises a fully representative distribution network, including the capabilities summarized in Table 6.1 This enables the research, test and demonstration of hardware, software and integrated systems solutions in a safe, controlled environment.

Table 6.1 Selected hardware and software assets of PNDC

Asset	Rating / Comments
11kV overhead/underground distribution	Up to 60kM of representative 11kV network
400V low voltage distribution	Up to 6kM of representative LV network
Controllable Motor-Generator (MG) set	1MW Motor / 5MVA Generator
Controllable load banks	600kVA controllable resistive/inductive
Real Time Digital Simulator (RTDS)	6 racks of RTDS execution hardware
Power Hardware in the Loop (PHIL)	540kVA bi-directional power converter
Distributed Energy Resources (DERs)	E.g., EV charge points, PV inverters, loads
Distribution Management System	Operational GE PowerOn SCADA
Data Acquisition System	Fluke & Beckhoff monitoring and logging

6.3.1. Overview of PEV Research and Testing Projects at PNDC

In 2019/20, the PNDC supported Power Line Technologies Ltd. (PTL), Chronos Technology Ltd, and the University of Strathclyde with development of the ENERSYN platform, which enables the hosting of partner developed applications. The platform monitors the low voltage (LV) network via high fidelity voltage and current measurements, making this data available to hosted 'apps'. Two apps developed were a micro Phasor Measurement Unit (PMU) and a Non-Intrusive Load Monitoring (NILM) algorithm, to detect the connection of electric vehicles (EV) to their chargers. The NILM algorithm uses machine learning techniques applied to LV network data to detect unique features related to EV charger operation. The test setup was varied in two ways. The first variation involved the Enersyn platform monitoring a rapid EV charging load isolated from background noise. The second variation involved monitoring a rapid EV charging load with other background loads supplied from the same distribution

circuit. A high-level representation of the setup is illustrated in Figure 6.3. Rogowski coil current transducers are installed on the incoming cables to the distribution board, and voltage transducer measurements taken off terminals inside the building's distribution board. Conducting testing with and without background load permitted the assessment of the NILM algorithm and its ability to disaggregate system noise from loads of interest.

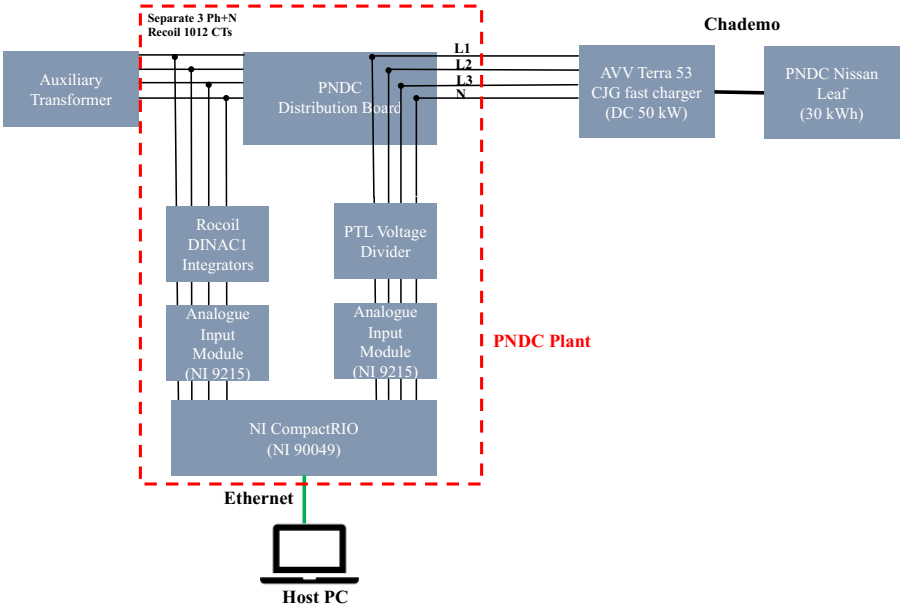

Figure 6.3 Iteration of test equipment and facility setup at the PNDC for NILM testing

The ENERSYN platform and an off-the-shelf data acquisition system were deployed in parallel to ensure the accuracy of data capture. Data was recorded using a National Instruments CompactRIO (NI CRIO) data acquisition system and a LabVIEW Virtual Instrument (VI) hosted on a PC. Three analogue input modules were deployed, with 4 channels per module. The other module employed in this setup was a global positioning system (GPS) time synchronization module. Data was sampled at a rate of 100kHz to provide a high-resolution data set for the development of machine learning features that underpin the NILM algorithm. Concurrent, PTL, Chronos and University of Strathclyde deployed the developed ENERSYN monitoring platform. The developed system incorporates current and voltage measurements

and records high-speed waveform events (100 kHz sampling rate) which are time stamped using GPS. The ENERSYN platform uses a long range (LoRa) GPS timing module supplied by Chronos. Captured waveform events are then analysed by the on-board micro-Phasor Measurement Unit (PMU) and passed to the Non-Intrusive Load Monitoring (NILM) algorithm (depicted in Figure 6.4). Noteworthy waveform events are flagged and forwarded onto the ENERSYN server for further analysis.

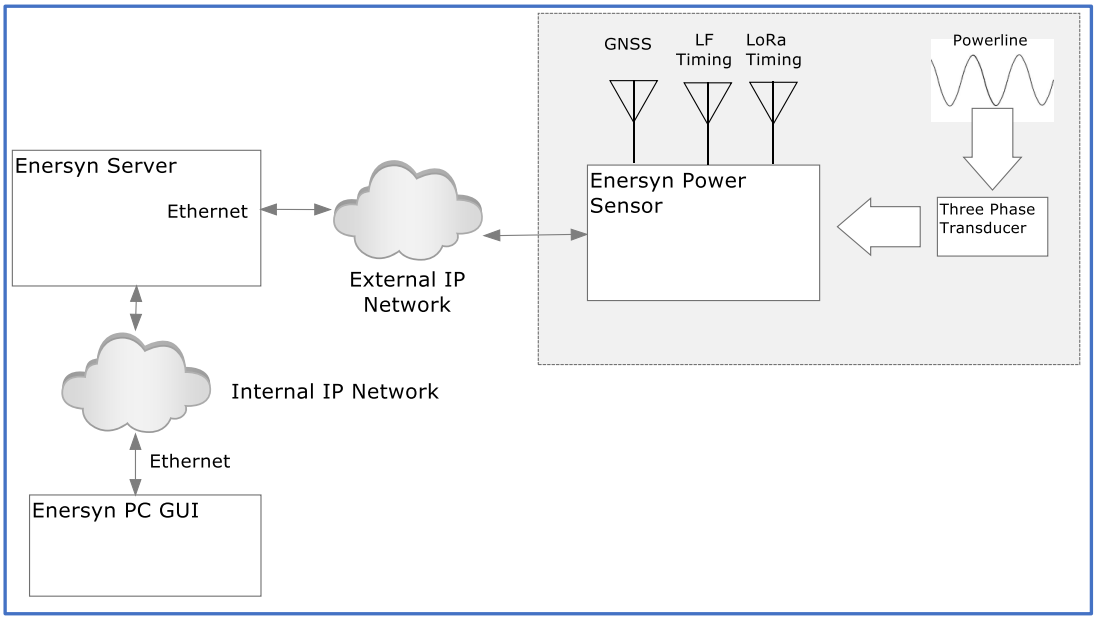

Figure 6.4 ENERSYN platform block diagram.

6.3.2. Summary of Results

High-resolution load signatures for a range of PEV charging profiles were analysed using data gathered by the National Instruments CRIO monitoring system. Previous studies (P. Zhang, 2011) have established a set of general usage patterns for charging PEVs, enabling four prescribed charging schedules to be derived, as illustrated in Figure 6.5, Figure 6.6, Figure 6.7 and Figure 6.8. These prescribed profiles were recreated, using PNDC owned electric vehicles, and used as inputs to the development of the NILM algorithm.

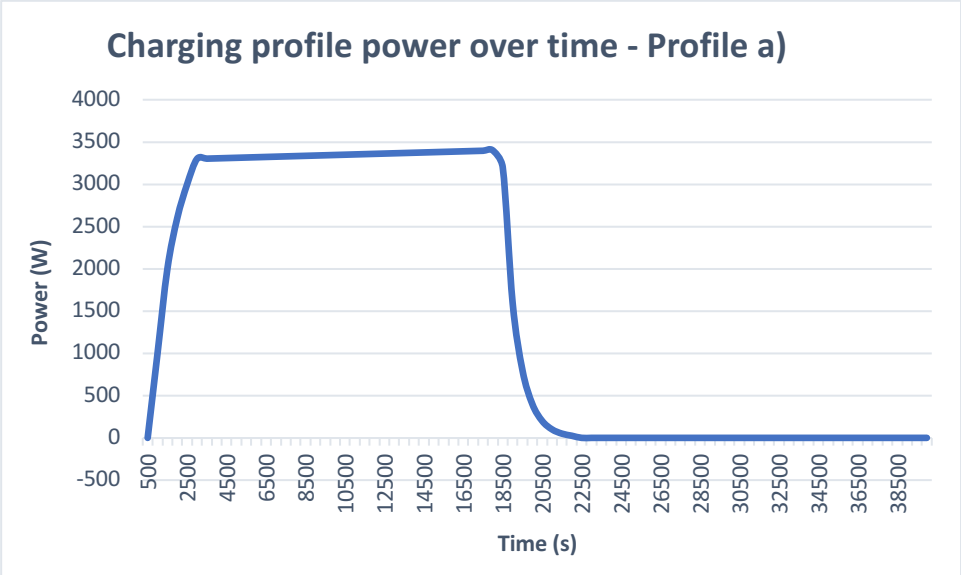

Figure 6.5: Profile a) empty to full (0 to 100%)

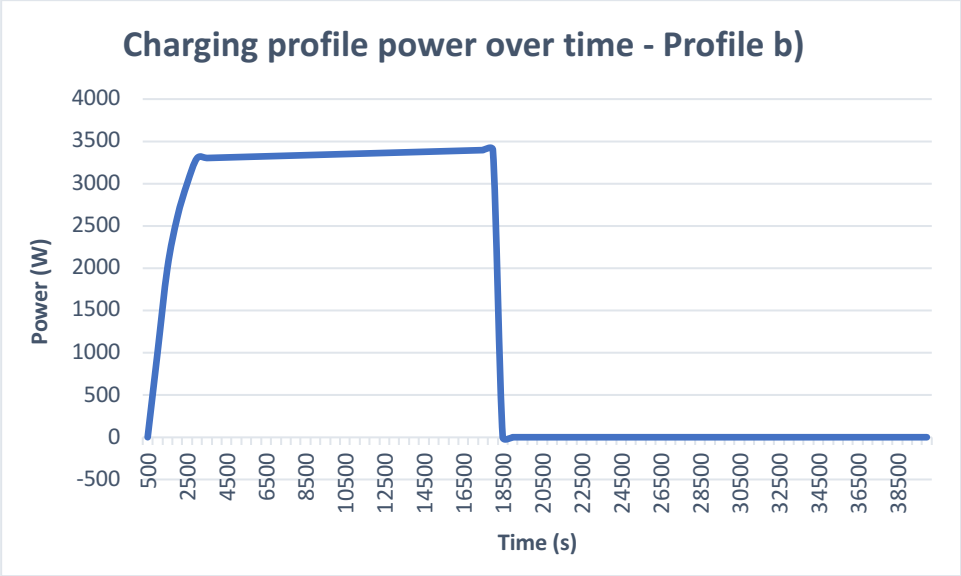

Figure 6.6: Profile b) empty to part full (0 to 75%)

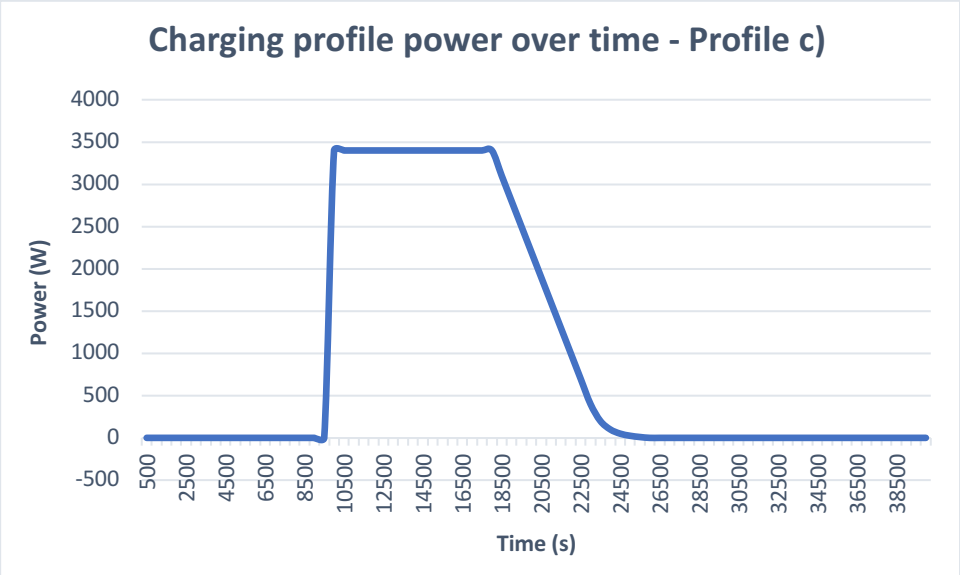

Figure 6.7: Profile c) part full to full (25 to 75%);

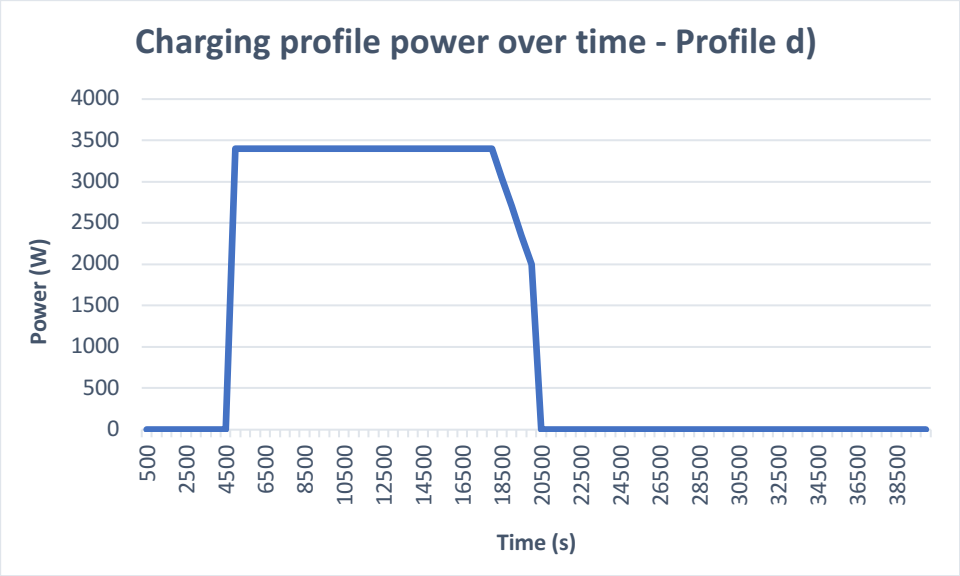

Figure 6.8: Profile d) part full to another higher capacity (25 to 75%)

PEV charger behaviour for non-prescribed charging profiles was also investigated by logging the electrical parameters on a public rapid 50kW charger. The logged data was correlated to voluntary questionnaire responses by charge point users about the start and end state of charge of their charging session. Figure 6.9 outlines the responses received, each point corresponding to a charge start and stop percentage.

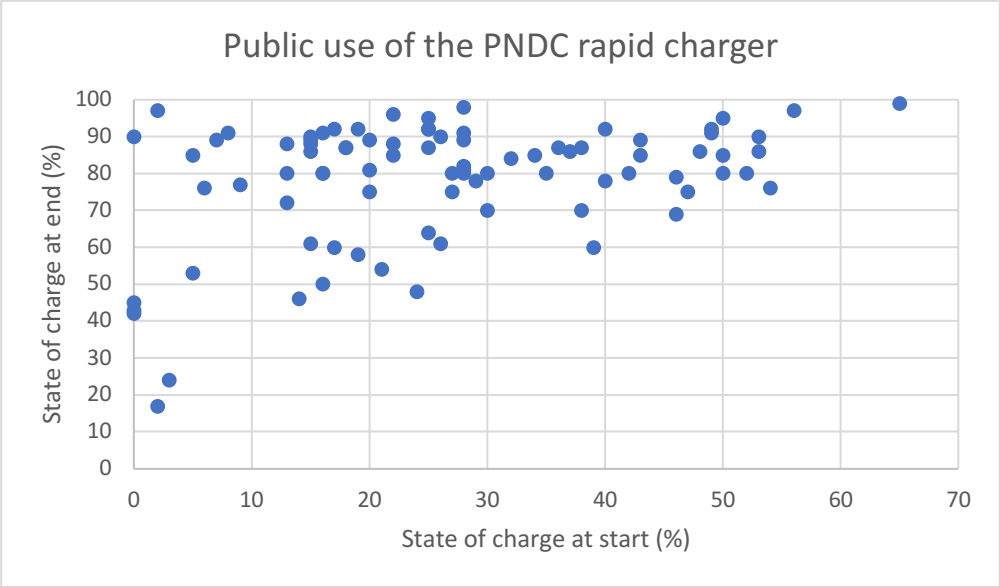

Figure 6.9 Public responses for usage of the PNDC rapid charger

Based on public responses, the majority of charging sessions started at 10 to 30 % state of charge (SOC) and stopped in the range of 70 to 100% SOC. This additional step provided inputs to ensure that the data for training the NILM algorithm was representative of how typical PEV drivers use public rapid chargers, in addition to the prescribed profiles found in literature Training data for the NILM algorithm was logged at a sampling frequency of 100 kHz, which was exported in a technical data management system (TDMS) format, compressed, and shared on a data storage platform with the project team. In terms of file size, a TDMS data file corresponding to 1 hours monitoring equated to 10 GB of data. This learning emphasised the need for on-board edge-processing analysis via the 'apps' on the ENERSYN platform, to avoid unnecessary data transmission to a server for centralized analysis.

The PEV charger data generated at the PNDC was critical to the NILM algorithm development. The PNDC is exploring further avenues of research which could make use of this high-fidelity data. The developed NILM algorithm is now operating at a success rate of over 90% in detecting PEV charger events after being trained and tested by the data gathered at PNDC. The

next stage of testing for the project will be the deployment of the ENERSYN platform on the PNDC test network and monitoring the public PEV chargers at PNDC over a longer period of time.

6.4. System Model

In this section, we consider a large-scale charging station with N chargers serving PEV demand. Charging station draws grid power and employs an on-site ESS shared by all users. We denote total charging power at time t by v_t and energy storage system (ESS) charge level is denoted by $i(t)$ fir $t \in \mathbb{R}^+$. It is worth noting that grid power is used to charge vehicles and storage unit whenever possible. When total PEV demand is higher than v_t, then ESS is used to support PEV demand unless it is fully empty. Customer statistics are as follows. We assume that PEVs' arrivals at parking station is a Poisson process with rate λ. The average parking duration follows an exponential distribution with rate μ (P. Fan, Operation analysis of fast charging stations with energy demand control of electric vehicles, 2015). Furthermore, when a vehicle is parked, its power demand follows Poisson process with rate β. Finally, when an arriving customer finds all system resources in use, then an outage event occurs. In our model, we use outage probability as the natural performance metric.

Since PEV arrivals are independent of each other, the system state space $\{0,1,\dots,N\}$ is represented with a birth-death process. The composite model for N slot charging station is depicted in Figure 6.10.

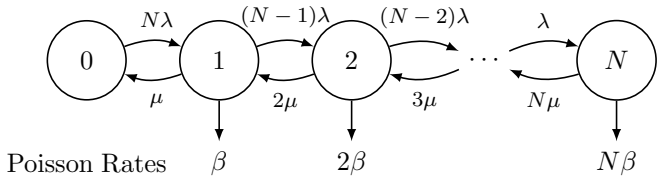

Figure 6.10: Birth-death process for N slot charging station

For the given system description, it is natural to assume that the system operates in a stable region. For this, the average demand should be strictly less than the available station capacity. To that end, we have

$$N\beta\left(\frac{\lambda}{\lambda+\mu}\right) < \nu_t, \tag{6.1}$$

or (6.1) can be rewritten as

$$\rho \equiv N\beta\left(\frac{\lambda}{\lambda+\mu}\right)\frac{1}{\nu_t} < 1, \tag{6.2}$$

where ρ is the utilization parameter. Furthermore, the following assumptions are made for the storage unit. First, energy rating (in kWh) or the size of the energy storage is denoted by B. Second, energy storage efficiency (charge-discharge) is denoted by η which takes values between 0 and 1. Note that this parameter reflects the percentage of energy transfer after losses are excluded. Third, in actual energy storage systems, small percentage of energy is lost due to leakage. To simplify matters, dissipation losses are ignored.

During charging station operations, on-site storage unit's energy level changes at one the following cases:

- When the storage unit is entirely discharged, that is $i(t) = 0$, and the total demand is more than ν_t. In this case, rate of change in storage charge level would be zero.
- ESS is fully charged, i.e., $i(t) = 1$, and total demand is less than ν_t. Similar to the previous case, ESS charge level would not change.
- ESS is partially discharged, that is $0 < i(t) < 1$, with any level of system demand. In this case, ESS charge level would change commensurate to the difference between charging power and the system demand, that is, $\frac{di(t)}{dt} = \eta(\nu_t - \sum_n L_n(t))$, where $L_n(t)$ is the total demand when $n \in \{0, \dots, N\}$ chargers are on at time t.

It is noteworthy that due to probabilistic nature of the system, by choosing storage size B, only probabilistic guarantees can be provided to system reliability. Therefore, let us define ε as the outage storage capacity, i.e., $B(\varepsilon)$, as the minimum B satisfies to serve $(100 - \varepsilon)\%$ per cent of the total load, i.e.,

$$B(\varepsilon) = \begin{cases} \min B \\ \text{subject to } \mathbb{P}(i(t) \geq B) \leq \varepsilon \end{cases}. \tag{6.3}$$

Note that our main goal is to calculate $\varepsilon -$ outage storage capacity $B(\varepsilon)$ based on grid power, the number of PEVs, and other system parameters. To simplify mathematical notations, ESS size is scaled and instead of B/η, we redefine B as the storage size. Furthermore, power systems planning is typically done for "peak hour" period. Therefore, in the rest of the paper, time index t is dropped and carry out calculations for the peak statistics.

6.4.1. Markov-modulated Poisson Process

Recall from the preceding discussion that at each state (see Figure 6.10) the aggregate demand generates state-dependent Poisson process (e.g., $\beta, 2\beta,$ etc.). Therefore, entire charging station can be modeled with a Markov-modulated Poisson Process (MMPP) and energy storage sizing option will be coupled with computation of steady state distribution probabilities. Let p_{in} denote the joint probability that the storage charge level is i and there are n active PEVs, that is

$$\mathrm{p_{in}} = \mathbb{P}(\text{ESS charge level=i, n active customers}). \tag{6.4}$$

Then, the probability that ESS charge level is at level i can be written as

$$p_i = \sum_{n=0}^{N} p_{in}. \tag{6.5}$$

Given the aforementioned assumptions, the system is modeled with a two-dimensional birth-death process as depicted in Figure 6.11. Note that system states of the Markov chain are represented by a doublet (i, n) where the first dimension reflects storage charge level and varies from 0 to B and the second dimension represents number of PEVs in the system and varies

from 0 to N. Alternatively, when customers arrive at or depart from the station, system state moves in the horizontal direction. Similarly, when the on-site storage is charged or discharged, system state moves in vertical direction. Moreover, transition rates e.g., λ, μ, etc. are determined based on the Poisson assumptions made earlier. It is worth emphasizing that storage sizing calculations are made based on the assumption that the storage size has an infinite capacity and the overflow probability calculated as given in (6.3).

6.4.2. Matrix Geometric Approach

To compute steady-state probabilities of the MMPP model, an algorithmic solution technique called matrix geometric approach has been employed (Neuts, 1994). As a first step, balance equations for the Markov chain is written in the form of (6.4). For instance, the last raw ($i = 0$), there are three intervals, (i) $i = 0, n = 0$, (ii) $i = 0, 1 \leq n \leq N - 1$, and (iii) $i = 0, n = N$.

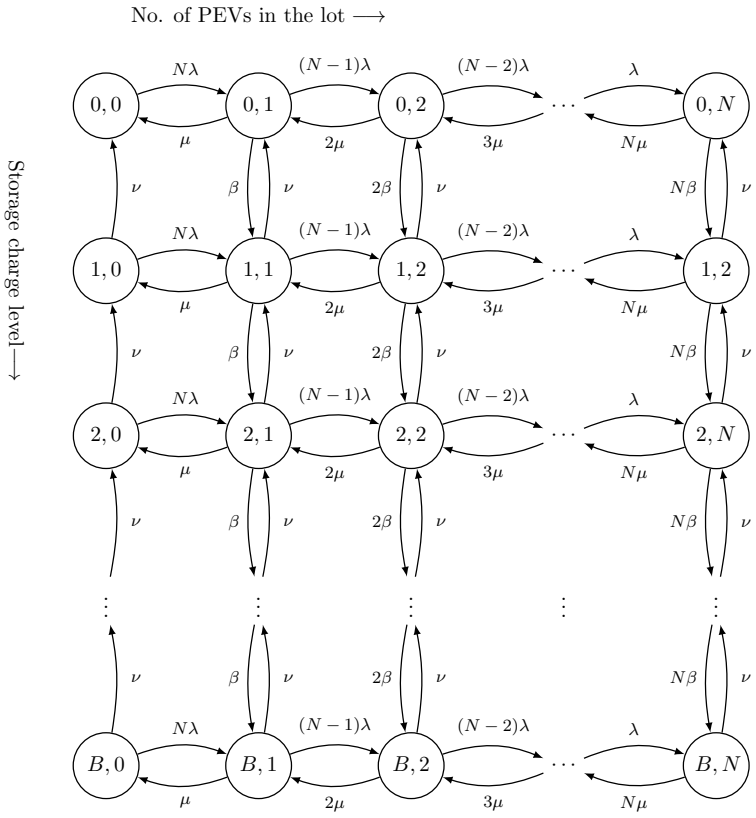

Figure 6.11: An illustrative MMPP model for the charging station with storage size B.

Vertical state transitions represent energy storage charge-discharge events, while horizontal ones depicts PEV arrival and departure.

For the first interval, the balance equation is

$$N\lambda p_{00} = \mu p_{01} + \nu p_{10}. \tag{6.6}$$

This equation can be rewritten as

$$p_{00} = (1 - N\lambda)\mu p_{01} + \nu p_{10}. \tag{6.7}$$

For the second interval, the balance equation can be rewritten as

$$\mathrm{p_{0n}} = \big(\mathrm{N} - (\mathrm{n}-1)\big)\lambda \mathrm{p_{0n-1}} + (1 - (\mathrm{N}-\mathrm{n})\lambda - \mathrm{n}\mu - \mathrm{n}\beta)\mathrm{p_{0n}} + (\mathrm{n}+1)\lambda \mathrm{p_{0n+1}} \nu \mathrm{p_{1n}}. \tag{6.8}$$

The third case includes the rightmost boundary states the balance equation can be rewritten as

$$\mathrm{p_{0N}} = \lambda \mathrm{p_{0N-1}} + (1 - \mathrm{N}\lambda - \mathrm{N}\beta)\mathrm{p_{0N}} + \nu \mathrm{p_{1N}}. \tag{6.9}$$

Balance equations for other rows e.g., $i > 0$, can be written similar to (6.7), (6.8), and (6.9) by further incorporating additional vertical state transitions. Let $\boldsymbol{p_i}$ denote $(N+1)$-element row vector compromised of probabilities defined by balance equations, that is $\boldsymbol{p_i} \equiv [p_{i0}, p_{i1}, \dots, p_{iN}]$. Then, balance equations, such as the ones defined in (6.7), (6.8), and (6.9), can be written in a compact matrix-vector equation. For $\boldsymbol{p_0}$,

$$\mathbf{p_0} = \mathbf{p_0} B_0 + \mathbf{p_1} \mathrm{B_1}, \tag{6.10}$$

where $(N+1)x(N+1)$ matrices B_0 and B_1 are readily given by

$$B_0 = \begin{bmatrix} (1-N\lambda) & N\lambda & 0 & \cdots & 0 \\ \mu & (1-\mu-(N-1)\lambda-\beta) & (N-1)\lambda & \cdots & 0 \\ 0 & 2\mu & (1-2\mu-(N-2)\lambda-2\beta) & \cdots & 0 \\ \vdots & \vdots & \vdots & \ddots & \vdots \\ 0 & 0 & 0 & \cdots & (1-N\mu-N\beta) \end{bmatrix} \tag{6.11}$$

and B_1 is a diagonal matrix the elements of which are composed of vertical transition rate ν. Remaining rows, e.g., $i > 0$ can be written similar (6.11) by including transitions between

vertically adjacent states. Hence, a complete set of balance equations for the remaining rows can be constructed from the matrix recurrences relation with three matrices such as A_0, A_1, and A_3, that is

$$\boldsymbol{p_i} = \boldsymbol{p_{i-1}}A_0 + \boldsymbol{p_i}A_1 + \boldsymbol{p_{i+1}}A_2 \text{ , for } i > 0 \tag{6.12}$$

Recall the assumption that the energy storage is initially assumed to have infinite size. Then, an infinite-dimension equation $\boldsymbol{p}$ is introduced as $\boldsymbol{p} = [\boldsymbol{p_0}, \boldsymbol{p_1}, \dots, \boldsymbol{p_i}, \dots]$. Then from (6.12), it is easy to see that

$$\boldsymbol{p} = \boldsymbol{p}P, \tag{6.13}$$

where matrix P is a stochastic matrix of infinite size and called as the transition probability matrix with each row summing to one. It is trivial that matrix P is concatenated from previously constructed submatrices, namely A_0, A_1, A_2, B_0, B_1, in the following repetitive form

$$P = \begin{bmatrix} B_0 & A_0 & 0 & 0 & \cdots \\ B_1 & A_1 & A_0 & 0 & \cdots \\ 0 & A_2 & A_1 & A_0 & \cdots \\ 0 & 0 & A_2 & A_1 & \cdots \\ 0 & 0 & 0 & A_2 & \cdots \\ \cdots & \cdots & \cdots & \cdots & \ddots \end{bmatrix} \tag{6.14}$$

In the next section, we present the solution methodology to compute minimum i that satisfies $\epsilon = 1 - \sum_i p_i$.

6.4.3. Algorithmic Solution Technique

In this section, the algorithmic probability solution developed by Neuts in (Neuts, 1994) is adopted. The solution to p_i is written as

$$p_{i+1} = p_i \mathrm{R}, \mathrm{i} \geq 0, \tag{6.15}$$

where R is a $(N+1)x(N+1)$ matrix has a non-negative solution to the following matrix equation

$$R = \sum_{k=0}^{\infty} R^k A_k. \tag{6.16}$$

Note that calculation of p_i is equivalent to finding the minimal nonnegative solution to R matrix. A recursive calculation method is used to compute the matrix R. As a first step, (6.16) is rewritten as

$$R[I - A_1] = \sum_{\substack{k=0 \\ k \neq 1}}^{\infty} R^k A_k \tag{6.17}$$

where I is an identitity matrix of $(N+1)x(N+1)$ size. Multiplying both sides of (6.17) would yield

$$R = \sum_{\substack{k=0 \\ k \neq 1}}^{\infty} R^k A_k \, [I - A_1]^{-1}. \tag{6.18}$$

R can be iteratively solved for an initial solution of $R = 0$,

$$R = [A_0 + R^2 A_2][I - A_1]^{-1}. \tag{6.19}$$

Once R is found, p_0 can be calculated by solving

$$p_0 = p_0 B(R), \tag{6.20}$$

where $B(R) = \sum_{k=0}^{\infty} R^k B_k$. Recall that for the charging station model, $B(R) = B_0 R B_1$. It is important to note that sum of probabilities should add up to 1. Once, the probabilities are found (e.g., p_0), the computed results need to be normalised by dividing each probability to sum of all probabilities. To that end, matrix geometric solution can be summarized as below:

1. Construct matrix R by solving the equation in (6.16) and iteration in (6.19)
2. Compute p_0 by solving the eigenvector equation in (6.20)
3. Compute p_i by solving (6.15)
4. Normalize p_0 and p_i by dividing by sum of all probabilities
5. Calculate minimum storage size that satisfies $\epsilon = 1 - \sum_i p_i$.

Case studies presented in the next section to provide more insights.

6.5. Numerical Evaluations

6.5.1. Computation of Station Parameters

Next, a number of case studies are presented to show how the proposed methodology can be used to size ESS sizing in a charging point. It is assumed that charging station employs typical level 2 chargers (6 kW), average parking duration is et as one hour ($\mu = 1$), and charge request is set to $\beta = 0.9$. Three levels of customer arrival rate per charger are chosen (from $\lambda = 0.25$ to $\lambda = 0.75$) to reflect different traffic regimes, while station size is varied from $N = 50$ to $N = 150$. For system's stability, (see equation (6.1)) the power drawn from the grid is chosen as

$$\nu = \mathrm{N}\beta\left(\frac{\lambda}{\lambda+\mu}\right) + \Delta, \tag{6.20}$$

where Δ is a small constant set to 0.02. Computations for the size of on-site energy storage system with respect to different station sizes and traffic regimes are presented in Figure 6.12. As an example, for a charging station with 150 chargers and peak traffic regime of $\lambda = 0.50$, the size of the energy storage to provide 2% outage performances would be 128 kWh.

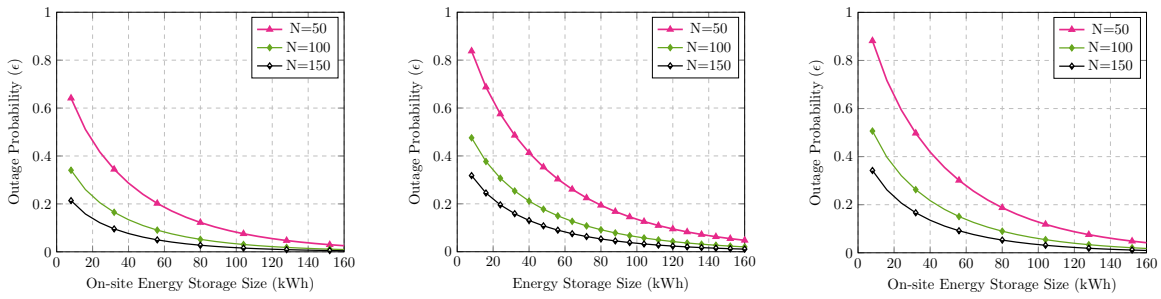

(a) Arrival rate $\lambda = 0.25N$ (b) Arrival rate $\lambda = 0.50N$ (c) Arrival rate $\lambda = 0.75N$

Figure 6.12 Computation of on-site energy storage size for different traffic regimes and station sizes

From the results presented in Figure 6.12 two key observations are made. First, as arrival rate increases, there is a need to a bigger energy storage to provide the same level of outage performance. Second, as the station size increases the need for storage size per charger decreases due to "statistical gains". For example, consider the following two charging stations with $N_1 = 50$ and $N_2 = 250$. Both stations operate under $\lambda = 0.5N$ and employ a storage size of $B = 112$kWh, while the station 2 draws three times more power than station 1, that is $\nu_2 = 3\nu_1$. For these two stations, outage probabilities are calculated as $\varepsilon_1 = 0.1093$ and $\varepsilon_2 = 0.0275$. Then, it is easy to see that gains in system performance ($\frac{\varepsilon_1}{\varepsilon_2} = 0.0275$) is higher the corresponding capacity increase ($\frac{\nu_1}{\nu_2} = 3.97$).

As a second evaluation, the case in which storage size and the number of chargers are known and the computation of the amount of power needed is investigated. In Figure 6.13, results for arrival rate $\lambda = 0.5$ and varying station sizes ($N = 100, 200,$ and 300) are presented. These findings help system operators to decide on appropriate amounts of power for the station. Similar to previous case, due to statistical gains, as the station size increases, per charger resource requirement decreases. For a target outage probability of 0.05 and on-site storage size of $B = 30$kWh, per charger power requirement for a $N = 100$ charging station is 4.69 kW, while this value is only 2.3 kW for a charging station with 300 slots.

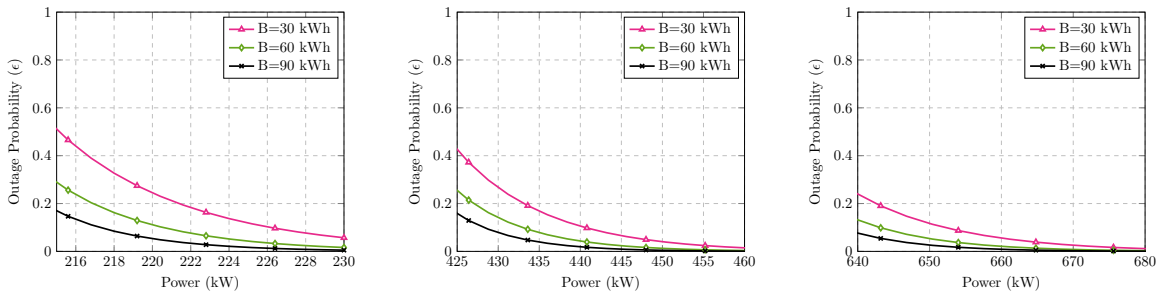

(a) Station Size $N = 100$ (b) Station Size $N = 200$ (c) Station Size $N = 300$

Figure 6.13 Energy storage size for varying grid power

6.5.2. Charging Station Economic Analysis

Recall that the principal motivation to acquire on-site energy storage systems at charging stations to lower running cost and defer major system upgrades. A typical electricity bill of a charging station is composed of three parts, namely (i) a fixed fee, (ii) energy charges (USD per kWh), and (iii) demand charges (USD per kW). In this case study, actual billing tariffs of a utility company in San Diego is employed with the following details. Monthly fee is $140, demand charge is $35 per highest kW, and energy tariffs are time of use based with details in Table 6.2.

Table 6.2. Electric vehicle charging tariffs (in US Cents per kWh) adopted from San Diego Gas and Electric Company

Time of Day	**Winter**	**Summer**
4 pm – 9 am	26	54
12 am – 6 am	9	25
10 am – 2pm	9	25
Other	25	30

It is assumed that the charging station operates between 6 am to 10 pm and hourly traffic demand per charger is in Table 6.3. Moreover, target outage probability is set to 0.005 and maximum grid power is limited to 610 kW.

Table 6.3. Hourly PEV demand per charger for the case study

Hour	**6 am**	**7 am**	**8 am**	**9 am**	**10 am**	**11 am**	**12 pm**	**1 pm**	**2pm**
Demand	0.2	0.3	0.4	0.5	0.6	0.7	0.7	0.8	0.9

Hour	3 pm	4 pm	5 pm	6 pm	7pm	8 pm	9 pm	10 pm	
Demand	0.8	0.7	0.7	0.6	0.5	0.4	0.3	0.2	

As a first step, energy storage size according to peak consumption hour is calculated using the methodology described in the previous section and found as $B = 108$ kWh. Next, amount of power needed to provide target outage probability is calculated and shown in Figure 6.14. The differences between the two curves relate to peak demand reduction enabled by employed energy storage unit. It can be observed from the presented results that station's peak demand is reduced by more than one third.

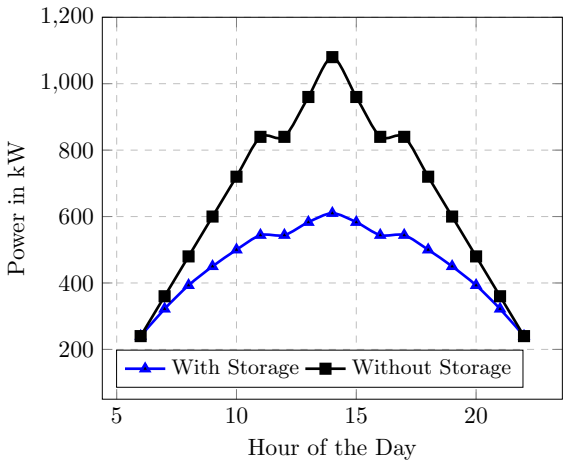

Figure 6.14 Hourly demand profile of the charging station

Now that necessary parameters are calculated, monthly electricity bill of charging station with and without an on-site energy storage is calculated for summer and winter tariffs.

Table 6.4 Comparison of monthly electricity bills (in thousands USD)

	Summer Tariff	**Winter Tariff**
With Storage	106.64	66.03
Without Storage	159	100.3

As presented in Table 6.4 employing an on-site storage reduces typically operational cost by 34% in winter and 33% in summer. To make a fair comparison, levelized cost of electricity (LCOE) which includes acquisition, operational expenses, and financial costs of storage unit needs to be included. According to a recent report (Henze, 2019) LCOE for lithium ion batteries has dropped to $187 per MWh. In this case study, the employed storage unit has a size of 106 kWh, hence the LCOE would be close to $18.7. By further incorporating this cost in the presented results, it can be concluded that employing storage units makes economic sense for charging station operators.

6.6. Conclusions

In this chapter, we have presented a probabilistic capacity planning approach for PEV charging stations equipped with an on-site ESS. The system is modelled with Markov-modulated Poisson process where each system state is represented by the number of customers in the station and energy storage charge level. To solve steady state probability distributions, an algorithmic solution technique (matrix-geometric) was adopted. The principal goal was to compute minimum energy storage size that can provide a good level of QoS measured by probability of outage events. In the last part, a number of case studies were presented to provide insights on how the model can be used in capacity planning. The results also showed that on-site storage systems can significantly lower station's peak demand and associated demand charges.

Acknowledgement

The ENERSYN project was funded by the European Space agency (ESA) via the Navigation Innovation and Support Programme (NAVISP) with programme code NAVISP-EL2-012 (ENERSYN project and funding, n.d.).

Bibliography

A. Khaligh, S. D. (2012). Comprehensive topological analysis of conductive and inductive charging solutions for plug-in electric vehicles . *IEEE Transactions on Vehicular Technology, 61*(8), 3475–3489.

Aveklouris, A. N. (2017). Electric vehicle charging: a queueing approach. *ACM SIGMETRICS Performance Evaluation Review,.*

Bayram IS, M. G. (2013). Electric power allocation in a network of fast charging stations. *IEEE Journal on Selected Areas in Communications, 31*(7), 1235-46.

Bayram, I. S. (2014). Unsplittable load balancing in a network of charging stations under QoS guarantees. *IEEE Transactions on Smart Grid, 6*(3), 1292-1302.

Cross, J. a. (2016). My Electric Avenue: Integrating electric vehicles into the electrical networks. *6th Hybrid and Electric Vehicles Conference.*

D. Ronanki, S. S. (2018). Modular multilevel converters for transportation electrification: challenges and opportunities. *IEEE Transactions on Transportation Electrification, 4*(2), 399–407.

E. Ucer, I. K. (2019). Modeling and analysis of a fast charging station and evaluation of service quality for electric vehicles. *IEEE Transactions on Transportation Electrification, 5*(1), 215–225 .

ENERSYN project and funding. (n.d.). Retrieved from https://navisp.esa.int/project/details/26/show

Falvo, M. S. (2014). EV charging stations and modes: International standards. *International Symposium on Power Electronics, Electrical Drives, Automation and Motion*, (pp. 1134-1139). Ischia, Italy.

Fotouhi, Z. H. (2019). 2019. A General Model for EV Drivers' Charging Behavior. *IEEE Transactions on Vehicular Technology, 68*(8), 7368-7382.

G. Fitzgerald, C. N. (2017). Evgo fleet and tariff analysis. Rocky Mountain Institute .

Han, S. H. (2010). Development of an optimal vehicle-to-grid aggregator for frequency regulation. *IEEE Transactions on smart grid, 1*(1), 65-72.

Haslett, A. (2019). *Smarter Charging-A UK Transition to Low Carbon Vehicles: Summary Report.* Loughborough: Energy Technologies Institute.

Henze, V. (2019). *Battery Power's Latest Plunge in Costs Threatens Coal, Gas.* New York: Bloomberg.

https://www.iea.org/reports/global-ev-outlook-2019. (2019). *Global EV Outlook.* International Energy Agency.

Hu, J. H. (2016). Electric vehicle fleet management in smart grids: A review of services, optimization and control aspects. *Renewable and Sustainable Energy Reviews, 56* , 1207-1226.

Bayram, I. S. (2019). A stochastic model for fast charging stations with energy storage systems. *IEEE Transportation Electrification Conference and Expo.* Novi, Michigan.

J. García-Villalobos, I. Z. (2014). Plug-in electric vehicles in electric distribution networks: A review of smart charging approaches. *Renew. Sustain. Energy Rev. , 38*, 717–731.

Jurgen Weiss, M. H. (2019). *Increased Transmission Investment to Support Growing Electrification Demand and Access Low-Cost Resources Can Reduce Customer Rates.* Brattle Group.

Lee, Z. L. (2019). ACN-Data: Analysis and Applications of an Open EV Charging Dataset. *Proceedings of the Tenth ACM International Conference on Future Energy Systems.*

M. R. Sarker, H. P.-V. (2018). Optimal operation of aggregated electric vehicle charging stations coupled with energy storage. *IET Generation, Transmission Distribution, 12*(5), 1127–1136.

M. Yilmaz, P. T. (2012). Review of battery charger topologies, charging power levels, and infrastructure for plug-in electric and hybrid vehicles. *IEEE transactions on Power Electronics , 28*(5), 2151–2169.

Neuts, M. F. (1994). *Matrix-geometric solutions in stochastic models: an algorithmic approach* . Courier Corporation.

P. Fan, B. S. (2015). Operation analysis of fast charging stations with energy demand control of electric vehicles. *IEEE Transactions on Smart Grid , 6*(4), 1819–1826.

Cong, C, Bayram I S, Devetsikiotis, M (2015). Revenue Optimization Frameworks for multi-clas sPEV charigng stations, . *IEEE Access, 3*, 2140-2150.

P. Zhang, C. Z. (2011). An Improved Non-Intrusive Load Monitoring Method for Recognition of Electric Vehicle Battery Load. *Energy Procedia , 12*, 104-112.

Power Networks Demonstration Centre. (n.d.). Retrieved February 2020, from https://pndc.co.uk/

S. Negarestani, M. F.-F.-G. (2016). Optimal sizing of storage system in a fast charging station for plug-in hybrid electric vehicles. *IEEE transactions on transportation electrification, 2*(4), 443–453.

S. S. Williamson, A. K. (2015). Industrial electronics for electric transportation: Current state-of-the-art and future challenges. *IEEE Transactions on Industrial Electronics, 62*(5), 3021–3032.

Sperling, D. (2018). Electric vehicles: Approaching the tipping point. In *Three Revolutions* (pp. 21-54). Washington DC: Island Press.

Srdic, S. a. (2019). Toward extreme fast charging: Challenges and opportunities in directly connecting to medium-voltage line. *IEEE Electrification Magazine, 7*(1), 22-31.

Tajer, I. S. (2017). *Plug-in Electric Vehicle Grid Integration.* London: Artech House.

Tehrani, N. a. (2015). Probabilistic estimation of plug-in electric vehicles charging load profile. *Electric Power Systems Research, 124*, 133-143.

(2018). *The 50 states of electric vehicles.* Raleigh, NC: NC Clean Energy Technology Center.

X. Liang, S. S. (2019). A 12.47 kv medium voltage input 350 kw ev fast charger using 10 kv sic mosfet. *IEEE Applied Power Electronics Conference and Exposition (APEC).*

Y. Liu, Y. Z. (2019). Challenges and opportunities towards fast-charging battery materials. *Nature Energy, 4*(7), 540–550.